

Cite this: *Chem. Commun.*, 2011, **47**, 11044–11046

www.rsc.org/chemcomm

COMMUNICATION

Nonheme ferric hydroperoxo intermediates are efficient oxidants of bromide oxidation†

Anil Kumar Vardhaman,^a Chivukula V. Sastri,^{*a} Devesh Kumar^{*b} and Sam P. de Visser^{*c}

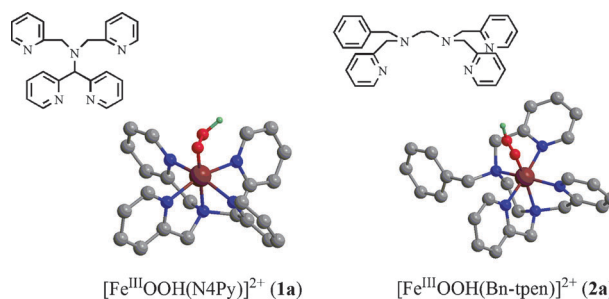
Received 24th June 2011, Accepted 24th August 2011

DOI: 10.1039/c1cc13775a

This work presents the first combined experimental and computational study that gives evidence of the electrophilic reactivity of a nonheme iron(III)-hydroperoxo species. We show that in contrast to their heme counterparts the nonheme iron(III)-hydroperoxo complexes are catalytically much more active and even more so than nonheme iron(IV)-oxo species.

Oxygen atom transfer reactions are vital processes in biosystems and take part in biodegradation, biosynthesis and bioconversion reactions in the body. Many of the enzymes utilize molecular oxygen on an iron center and, for instance, contain the class of cytochrome P450 enzymes (P450s), which is a versatile group of enzymes involved in drug metabolism, hormone biosynthesis and detoxification processes.¹ The active species of the P450s is an iron(IV)-oxo heme cation radical (Compound I, Cpd I) and its precursor in the catalytic cycle is the iron(III)-hydroperoxo species (Compound 0, Cpd 0). Cpd I and Cpd 0 have both been characterized with spectroscopic methods and are relatively short-lived.² Reactivity studies together with supporting computational modeling provided evidence, however, that only Cpd I is an active oxidant of oxygen atom transfer reactions, while Cpd 0 is a sluggish oxidant.³

The nonheme iron chemistry of biomimetic systems and enzymes led to the characterization of a number of high-valent iron(IV)-oxo intermediates in electrophilic and nucleophilic oxygenation reactions.⁴ However, the reactivity patterns of the corresponding nonheme Fe(III)-hydroperoxo intermediates are not well understood. To gain insight into the reactivity patterns of nonheme Fe(III)-hydroperoxo intermediates in electrophilic reaction mechanisms, we decided to investigate the bromide



Scheme 1 Oxidants used in this study.

oxidation by $[\text{Fe}^{\text{III}}\text{OOH}(\text{N4Py})]^{2+}$ (**1a**) and $[\text{Fe}^{\text{III}}\text{OOH}(\text{Bn-tpen})]^{2+}$ (**2a**),⁵ Scheme 1, using combined experimental and computational techniques. These nonheme complexes contain pentadentate ligands and their corresponding iron(IV)-oxo complexes have been shown to give efficient electrophilic reactivity patterns with substrates including hydrogen atom abstraction mechanisms.⁶ Nam and co-workers studied **1a** and **2a** and found them to be inactive with thioanisole and cyclohexene.⁷

The ferric hydroperoxo complexes, **1a** and **2a**, were generated in a methanol solution *in situ* by adding excess H_2O_2 following a previously reported procedure.⁸ Subsequently, tetrabutyl ammonium bromide (TBABr) was added to the solution of **1a** at 253 K, which led to the rapid decay of the characteristic 548 nm peak in the UV-Vis spectra and the efficient formation of $[\text{Fe}^{\text{III}}(\text{OH})(\text{N4Py})]^{2+}$, see Fig. 1a. We evaluated the second order rate constant for this reaction to be $5.5 \times 10^{-1} \text{ M}^{-1} \text{ s}^{-1}$. This is a very fast reaction and is several orders of magnitude faster than, for instance, the same reaction catalyzed by the corresponding Fe(IV)-oxo complexes (**1b**) for which we determined a second order rate constant of $6.4 \times 10^{-4} \text{ M}^{-1} \text{ s}^{-1}$ using the same experimental conditions (Fig. 1b). This implies that the Fe(III)-hydroperoxo complex reacts with bromide with rate constants that are about three orders of magnitude higher than those found for the ferryl-oxo complex. To highlight the difference in reactivity between **1a** and **1b** with bromide we plot the rate constants of bromide oxidation at different concentrations in Fig. 1c. To find out whether the same rate enhancement is observed with other nonheme iron ligand systems, we investigated the same reactions for the iron(III)-hydroperoxo and iron(IV)-oxo species with the Bn-tpen ligand system: structures **2a** and **2b**, respectively. Indeed, a similar

^a Department of Chemistry, Indian Institute of Technology Guwahati, Assam 781039, India. E-mail: sastricv@iitg.ernet.in; Fax: +91-361-258-2349

^b Department of Applied Physics, School for Physical Sciences, Babasaheb Bhimrao Ambedkar University, Vidya Vihar, Rae Bareilly Road, Lucknow 226 025, India. E-mail: dkclere@yahoo.com

^c The Manchester Interdisciplinary Biocentre and the School of Chemical Engineering and Analytical Science, The University of Manchester, 131 Princess Street, Manchester M1 7DN, UK. E-mail: sam.devisser@manchester.ac.uk

† Electronic supplementary information (ESI) available: Detailed experimental and computational methods, tables with group spin densities, charges and absolute and relative energies of calculated structures. Also given are figures with optimized geometries, geometry scans and experimental data on **2a** and **2b**. See DOI: 10.1039/c1cc13775a

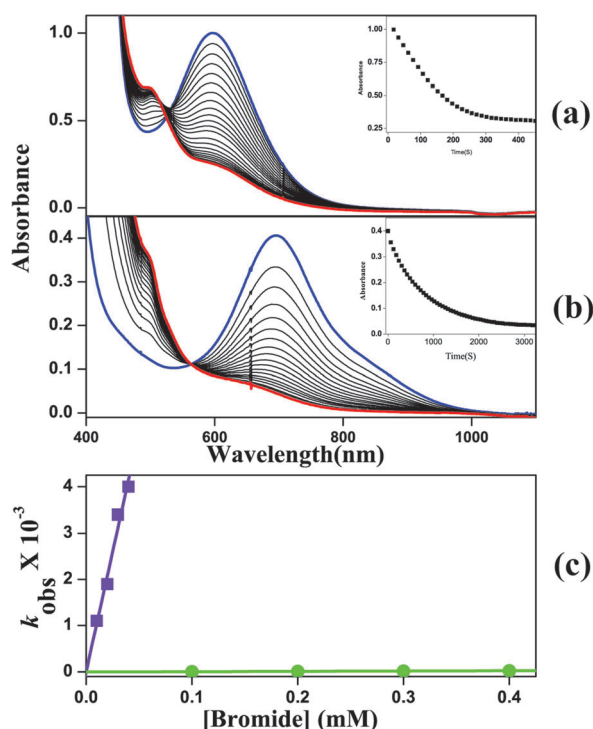


Fig. 1 UV-vis spectral changes of (a) **1a** (1 mM) upon addition of 10 equiv. of TBABr at 253 K. Scan interval was 10 s. The inset shows the time course of **1a** monitored at 548 nm. (b) **1b** (1 mM) upon addition of 10 equiv. of TBABr at 298 K. Scan interval was 10 s. The inset displays the time course of **1b** monitored at 695 nm. (c) Comparison of the second order rate constants of bromide oxidation by **1a**, $5.5 \times 10^{-1} \text{ M}^{-1} \text{ s}^{-1}$ (■), and **1b**, $6.4 \times 10^{-4} \text{ M}^{-1} \text{ s}^{-1}$ (●) with TBABr at 253 K.

enhanced bromide oxidation rate was observed for **2a** ($2.7 \times 10^{-1} \text{ M}^{-1} \text{ s}^{-1}$) as compared to **2b** ($1.0 \times 10^{-2} \text{ M}^{-1} \text{ s}^{-1}$) at 253 K, ESI†, Fig. S10. It should be noted here that the order of reactivity for the ferryl complexes was **2b** > **1b**, which is consistent with previous reactivity studies of these oxidants.⁶ By contrast, the reverse ordering was observed for the Fe(III)-hydroperoxo complexes, *i.e.* **1a** > **2a**.

To understand the apparent disparity between the reactivity of **1a/2a** on the one hand *versus* that of **1b/2b** on the other hand, as compared to what is known for heme-enzymes and biomimetic analogues, we monitored the product distributions of all processes. Thus, bromide oxidation of phenol red by a high-valent Fe(III)-hydroperoxo species leads to the production of bromophenol blue, or the tetrabrominated product of phenol red.⁹ However, in the presence of HOBr, Br₂ or Br₃[−], phenol red is easily tetra-brominated to form bromophenol blue. The addition of H₂O₂ to our solution containing [Fe^{II}(N4Py)]²⁺ (or [Fe^{II}(Bn-tpen)]²⁺) and phenol-red in the presence of excess TBABr resulted in a red-shift in the UV-Vis spectra from 441 nm (orange-red) to 590 nm (blue), indicative of the conversion from phenol red to bromophenol blue (Fig. 2). Similar results were obtained under inert conditions. The yield of bromophenol blue was ~80% based on the molar absorption coefficient of bromophenol blue and showed a time-dependent absorbance change, arising from the formation of bromophenol blue (inset, Fig. 2; ESI†, Fig. S11). As can be seen from Fig. 2, the bromophenol blue was initially produced slowly (long lag phase) due

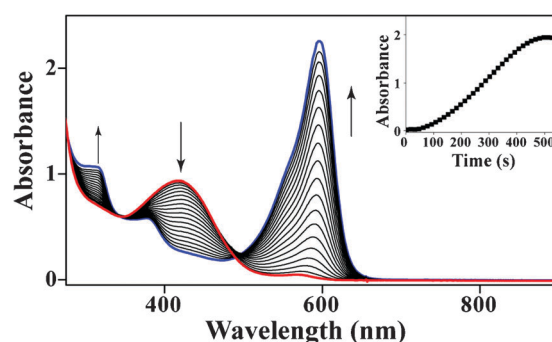


Fig. 2 Catalytic conversion of phenol red (62.5 μM) to bromophenol blue in the presence of [Fe^{II}(N4Py)]²⁺ (0.1 mM) and TBABr (80 mM) upon addition of H₂O₂ (10 mM). The inset shows the time course of formation of bromophenol blue monitored at 590 nm.

to the absence of BrO[−], but after the concentration of BrO[−] increases, so does the amount of bromophenol blue. However, when a steady-state concentration of BrO[−] is reached, the formation rate of bromophenol blue is equal to the rate of bromide oxidation by **1a**. The duration of the initial lag decreased with the increasing concentration of the catalyst. The systematic variation of the catalyst concentration and the measurements of the initial rate of bromophenol blue formation are found to be of first-order, which is in agreement with the results given above. The uncatalyzed bromide oxidation by H₂O₂ in the absence of a catalyst was reported to be in the order of $10^{-7} \text{ M}^{-1} \text{ s}^{-1}$.¹⁰

Due to the fact that **1a/2a** cannot be generated in an acetonitrile solution, whereas **1b/2b** cannot be studied in a methanol solution as a result of alcohol oxidation, the above mentioned experiments of **1a** vs. **1b** and **2a** vs. **2b** refer to studies in a different solvent. To confirm that **1a/2a** are better oxidants than **1b/2b** of bromination reactions we decided to run a series of density functional theory studies. Essentially, we do full geometry optimizations with the polarized continuum model with a dielectric constant of $\epsilon = 35.7$ (acetonitrile) or 32.6 (methanol) using previously described procedures.¹¹ Fig. 3 displays the free energy landscape for bromination with **1a** and **2a** as oxidants. Thus, the reaction is concerted *via* the bromination transition state TS_{Br} and leads to an Fe^{III}-hydroxo complex with nearby OBr[−] (**P**). The reactants have a sextet spin ground state, while the doublet and quartet spin states are 7.2/6.7 and 32.8/7.8 kcal mol^{−1} higher in energy.

The bromination reactions by **61a** and **62a** have free energies of activation of 21.8 and 27.1 kcal mol^{−1}, respectively. Using transition state theory the rate constant for **1a** reported in Fig. 1 corresponds to $\Delta G^\ddagger = 18.5 \text{ kcal mol}^{-1}$, therefore, we find good agreement between experiment and computation with similar ΔG^\ddagger differences as before.¹² We also calculated the bond dissociation energy of the O–O bond in **1a/2a** to give the corresponding iron(IV)-oxo complexes and found enthalpies that are 32/13 kcal mol^{−1} above those of **6TS1a/6TS2a**. Therefore, the observed products are due to reactivity of **1a/2a** and not from interconversion of **1a/2a** into **1b/2b** first. As can be seen from Fig. 3, the optimized geometries of TS_{Br,1a} and TS_{Br,2a} are very similar and consequently cannot be the origin of the difference in reaction barrier between the two processes.

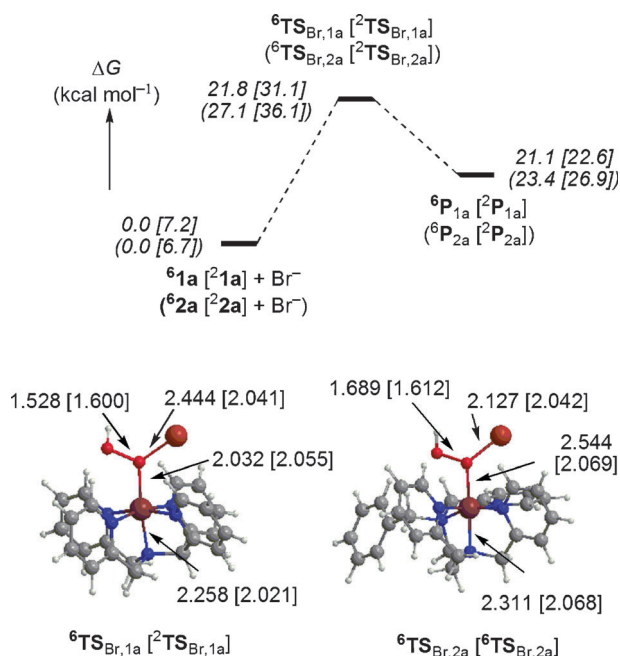
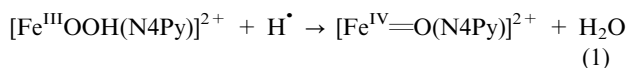


Fig. 3 DFT calculated mechanism of bromination by **1a** and **2a**. Free energies are reported in kcal mol^{−1} with energies and solvent corrections taken from the UB3LYP/B2//UB3LYP/B1 calculations and include zero point, thermal, and entropic corrections at UB3LYP/B1. Also given are optimized geometries of the TSs with bond lengths in angstroms.

The DFT calculations, therefore, do support the experimental observations of higher reactivity of **1a** over **2a** in bromination reactions.

The origin of the high reactivity of nonheme iron(III)-hydroperoxo can be traced to the orbital occupation. Thus, nonheme iron(IV)-oxo species are stabilized in high-spin states with an elevated π^*_{xy} orbital as compared to heme iron(IV)-oxo species.^{6b,13} The same is true for iron(III)-hydroperoxo that is low-spin in heme systems but high-spin in nonheme systems. These high-spin species are more reactive and can abstract hydrogen atoms/electrons more easily than their low-spin counterparts. To assess the oxidative potential of the iron(III)-hydroperoxo species, we calculate the reaction energy (BDE_{OH}) for reaction (1) using isolated molecules.



Thus, the calculated reaction energy starting from **1a** is 91.1 kcal mol^{−1}, while that from **2a** is found to be 85.6 kcal mol^{−1}. By contrast, the H-abstraction energy calculated for Cpd0 of P450 is only 81.2 kcal mol^{−1} due to two doubly occupied 3d-type orbitals.¹⁴ As shown previously, differences in BDE_{OH} values are proportional to H-abstraction rate constants and a larger BDE_{OH} value should correspond to faster reactions.¹⁵ Indeed the relative BDE_{OH} values for **1a** and **2a** follow the trend in barrier heights and rate constants discussed here. These BDE_{OH} values are close to those calculated for CpdI of P450 (88.9 kcal mol^{−1}),¹⁴ hence, in particular, **1a** should be an efficient oxidant of electrophilic reaction mechanisms.

We provide the first experimental and computational evidence that nonheme iron(III)-hydroperoxo species are efficient oxidants of electrophilic oxidation reactions. This makes nonheme iron(III)-hydroperoxo complexes fundamentally different from heme iron(III)-hydroperoxo species.

Research support was provided to CVS by Department of Science and Technology, India (SR/S1/IC-02/2009), and Board of Research in Nuclear Sciences, India (2010/37C/3/BRNS). CPU time was provided by the National Service of Computational Chemistry Software (NSCCS). DK acknowledges Department of Science and Technology (New Delhi) for the Ramanujan Fellowship.

Notes and references

- (a) M. Sono, M. P. Roach, E. D. Coulter and J. H. Dawson, *Chem. Rev.*, 1996, **96**, 2841; (b) J. T. Groves, *Proc. Natl. Acad. Sci. U. S. A.*, 2003, **100**, 3569; (c) *Cytochrome P450: Structure, Mechanism and Biochemistry*, ed. P. R. Ortiz de Montellano, 3rd edn, Kluwer Academic/Plenum Publ., New York, 2005.
- (a) R. Davydov, T. M. Makris, V. Kofman, D. E. Werst, S. G. Sligar and B. M. Hoffman, *J. Am. Chem. Soc.*, 2001, **123**, 1403; (b) P. J. Mak, I. G. Denisov, D. Victoria, T. M. Makris, T. Deng, S. G. Sligar and J. R. Kincaid, *J. Am. Chem. Soc.*, 2007, **129**, 6382; (c) J.-G. Liu, T. Ohta, S. Yamaguchi, T. Ogura, S. Sakamoto, Y. Maeda and Y. Naruta, *Angew. Chem., Int. Ed.*, 2009, **48**, 9262; (d) J. Rittle and M. T. Green, *Science*, 2010, **330**, 933.
- (a) F. Ogliaro, S. P. de Visser, S. Cohen, P. K. Sharma and S. Shaik, *J. Am. Chem. Soc.*, 2002, **124**, 2806; (b) S. Shaik, H. Hirao and D. Kumar, *Nat. Prod. Rep.*, 2007, **24**, 533; (c) S. P. de Visser, J. S. Valentine and W. Nam, *Angew. Chem., Int. Ed.*, 2010, **49**, 2099.
- (a) M. Costas, M. P. Mehn, M. P. Jensen and L. Que Jr, *Chem. Rev.*, 2004, **104**, 939; (b) M. M. Abu-Omar, A. Loaiza and N. Hontzeas, *Chem. Rev.*, 2005, **105**, 2227; (c) P. C. A. Bruijninx, G. van Koten and R. J. M. Klein Gebbink, *Chem. Soc. Rev.*, 2008, **37**, 2716; (d) L. Que Jr, *Acc. Chem. Res.*, 2007, **40**, 493; (e) W. Nam, *Acc. Chem. Res.*, 2007, **40**, 522.
- Abbreviations used: N4Py, *N,N*-bis(2-pyridylmethyl)-*N*-bis(2-pyridyl)-methylamine; Bn-tpen, *N*-benzyl-*N,N'*,*N'*-tris(2-pyridylmethyl)ethane-1,2-diamine.
- (a) J. Kaizer, E. J. Klinker, N. Y. Oh, J.-U. Rohde, W. J. Song, A. Stubna, J. Kim, E. Münck, W. Nam and L. Que Jr, *J. Am. Chem. Soc.*, 2004, **126**, 472; (b) D. Kumar, H. Hirao, L. Que Jr and S. Shaik, *J. Am. Chem. Soc.*, 2005, **127**, 8026; (c) C. V. Sastri, K. Oh, Y. J. Lee, M. S. Seo, W. Shin and W. Nam, *Angew. Chem., Int. Ed.*, 2006, **45**, 3992.
- M. J. Park, J. Lee, Y. Suh, J. Kim and W. Nam, *J. Am. Chem. Soc.*, 2006, **128**, 2630.
- (a) A. Hazell, C. J. McKenzie, L. P. Nielsen, S. Schindler and M. Weitzer, *J. Chem. Soc., Dalton Trans.*, 2002, 310; (b) K. D. Koehn, J.-U. Rohde, M. Costas and L. Que Jr, *Dalton Trans.*, 2004, 3191.
- Phenol red is commonly used as a standard assay for haloperoxidase activity, see e.g. J. V. Walker, M. Morey, H. Carlsson, A. Davidson, G. D. Stucky and A. Butler, *J. Am. Chem. Soc.*, 1997, **119**, 6921.
- M. S. Reynolds, S. J. Morandi, J. W. Raebiger, S. P. Melican and E. Smith, *Inorg. Chem.*, 1994, **33**, 4977.
- (a) D. Kumar, B. Karamzadeh, G. N. Sastry and S. P. de Visser, *J. Am. Chem. Soc.*, 2010, **132**, 7656; (b) D. Kumar, G. N. Sastry and S. P. de Visser, *Chem.-Eur. J.*, 2011, **17**, 6196.
- D. Kumar, S. P. de Visser and S. Shaik, *Chem.-Eur. J.*, 2005, **11**, 2825.
- S. P. de Visser, *J. Am. Chem. Soc.*, 2006, **128**, 15809.
- (a) S. P. de Visser, *Chem.-Eur. J.*, 2006, **12**, 8168; (b) S. P. de Visser and L. S. Tan, *J. Am. Chem. Soc.*, 2008, **130**, 12961.
- (a) J. M. Mayer, *Acc. Chem. Res.*, 1998, **31**, 441; (b) K. A. Prokop, S. P. de Visser and D. P. Goldberg, *Angew. Chem., Int. Ed.*, 2010, **49**, 6111; (c) S. P. de Visser, *J. Am. Chem. Soc.*, 2010, **132**, 1087.